Hydrogen Incorporation in Semiconductors

Norbert H. Nickel

In many materials, the presence of hydrogen influences the structural and electronic properties. An equilibrium model based on statistical mechanics is presented that describes the unintentional incorporation of hydrogen. As an example, the H concentration in four different semiconductors, namely, c-Si, c-Ge, ZnO, and β-Ga$_2$O$_3$, is measured using H effusion. The measured H concentration ranges from 5.2×10^{16} to 1.1×10^{18} cm^{-3}. From the effusion data, the position of the H chemical potential and the H binding energies are derived.

1. Introduction

Hydrogen, as the smallest and simplest atom, possesses properties that affect both the structural and electronic properties of solids. The role of hydrogen in metals and semiconductors has been studied extensively in the last decades.[1–7] For the chemical identification of H complexes in semiconductors, optical and magnetic resonance methods are often used. However, to obtain measurable signals the specimens have to be exposed to hydrogen to increase its concentration either by using posthydrogenation techniques or by using H containing precursors during growth. As a consequence, it is widely believed that untreated semiconductors do not contain hydrogen. This, however, is a fallacy as we show in this article.

The unintentional incorporation of hydrogen into semiconductors can occur at any production step starting with the high-temperature growth of crystals, followed by wafer dicing, etching, and polishing processes. This is related to the fact that hydrogen is present in each of the processing steps, e.g., as a component of the used etching and cleaning chemicals or as an impurity in the form of residual water vapor.[8,9] Consequently, even crystals of high purity contain a considerable amount of hydrogen. During crystal growth, H incorporation is driven by thermodynamics. The key quantities that drive

N. H. Nickel
Institut für Silizium-Photovoltaik
Helmholtz-Zentrum Berlin für Materialien und Energie GmbH
Schwarzschildstr. 8, 12489 Berlin, Germany
E-mail: nickel@helmholtz-berlin.de

The ORCID identification number(s) for the author(s) of this article can be found under https://doi.org/10.1002/pssb.202300309.

hydrogen incorporation into the lattice of a perfect solid are enthalpy and entropy. Equilibrium growth conditions yield H concentrations between 5.2×10^{16} and 1.1×10^{18} cm^{-3} in elemental semiconductors and wide bandgap oxides. The H binding energies are specific to each semiconductor and are presented as a hydrogen density-of-states.

2. Thermodynamic Approach

The equilibrium concentration of hydrogen atoms in a solid is governed by statistical mechanics. Let us consider a monatomic solid with N atoms at uniform pressure, p, and temperature, T, that can accommodate a number of n hydrogen atoms that can migrate in the host lattice but do not interact with each other. This assumption is justified because the hydrogen concentration in all investigated semiconductors is low (see experimental data below). At this point, we only consider uncharged H atoms. The Gibbs free energy of this system is given by

$$G(p, T) = G_0(p, T) + ng(p, T) - k_B T \ln\left(\frac{(N+n)!}{N!n!}\right) \quad (1)$$

where $G_0(p, T)$ is the Gibbs free energy of the perfect solid, $g(p, T)$ is the Gibbs free energy of the H sites in the solid, and the last term is the configurational entropy of n hydrogen atoms occupying $n + N$ sites.

Under equilibrium conditions, e.g., for constant temperature and pressure, the Gibbs free energy is minimized, and the corresponding hydrogen concentration can be obtained from

$$\mu_H \equiv \left(\frac{\partial G}{\partial n}\right)_{p,T} = 0 \quad (2)$$

Using the Stirling approximation for the partial derivative of the configurational entropy term, the hydrogen chemical potential is given by

$$\mu_H = g + k_B T \ln\left(\frac{n}{N+n}\right) \quad (3)$$

which contains a contribution from the crystal and the H atoms. Thus, for $n \ll N$, the concentration of hydrogen-occupied sites in the host lattice is given by

$$n \approx N \exp\left(-\frac{g}{k_B T}\right) \quad (4)$$

Hence, with increasing temperature, the H concentration increases exponentially.

In many semiconductors the lowest energy state of hydrogen is either H^+ or H^-. Also, the charge state of hydrogen depends on the position of the Fermi energy. As the Fermi energy moves from the valence to the conduction band, the charge state of hydrogen changes from H^+ to H^-.[10–12] In some materials such as ZnO, this transition occurs in the conduction band, e.g., in ZnO hydrogen is always positively charged.[10] Accordingly, the donor level resides above the acceptor level, which is characteristic for a system with a negative correlation energy.[10] Consequently, when hydrogen atoms migrate into a semiconductor the interaction with the electronic system has to be taken into account by considering one of the following two equilibrium reactions

$$H^0 \rightleftharpoons H^- + h$$
$$H^0 \rightleftharpoons H^+ + e \tag{5}$$

according to the position of the Fermi energy. Here, h and e represent holes and electrons, respectively. The ratio of the concentrations of H atoms in the different charge states is determined by the differences of the formation energies, ΔG_X. For negatively charged hydrogen atoms, this yields

$$\frac{C_{H^-}}{C_{H^0}} = \frac{\phi_{H^-}}{\phi_{H^0}} \exp\left(-\frac{\Delta G_{H^-} - \Delta G_{H^0}}{k_B T}\right) \tag{6}$$

where ϕ_{H^-} and ϕ_{H^0} describe the possible configurations of H^- and H^0. Since hydrogen interacts with the electronic system of the host lattice, the energy for removing an electron from, or donating an electron to the host lattice, is the Fermi energy, E_F. The energy of the electron added to the H atom is E_A. Hence, Equation (6) can be rewritten as

$$\frac{C_{H^-}}{C_{H^0}} = \frac{\phi_{H^-}}{\phi_{H^0}} \exp\left(\frac{E_F - E_A}{k_B T}\right) \tag{7}$$

For the donor state of hydrogen, an analogous equation can be derived where E_D denotes the energy of the electron donated to the host lattice. Hence, the incorporation of hydrogen into semiconductors influences the Fermi energy. In fact, in many semiconductors hydrogen counteracts the present doping.

Semiconductors are grown at high temperatures and under well-controlled conditions. Depending on the growth method, ultrapure materials such as crystalline germanium or float-zone silicon can be produced. However, despite all efforts it is unavoidable that hydrogen is incorporated into the crystals. One reason is the fact that residual water vapor is present even in well-baked vacuum systems. These molecules can dissociate thermally[13] and by electron impact[14] and, thus, are a source for hydrogen. Hence, during the growth of semiconductors, an equilibrium between the residual H concentration in the growth chamber and the solid is established. This leads to an equilibration of the hydrogen chemical potentials in the semiconductor and in the gas phase

$$\mu_H^{gas} = \mu_H \tag{8}$$

For monatomic hydrogen with an electron spin of $S = \frac{1}{2}$, the chemical potential is given by[15]

$$\mu_H^{gas} = k_B T \ln\left(\frac{C_H}{2n_q}\right) - k_B T \ln 2 \tag{9}$$

Here, C_H is the atomic hydrogen concentration, T is the temperature, and $1/n_q$ is the quantum volume defined as[15]

$$n_q = \left(\frac{mT}{2\pi h^2}\right)^{3/2} \tag{10}$$

where m is the mass of the hydrogen atom and h is the Planck constant. In **Figure 1** μ_H^{gas} is shown as a function of the gas temperature for H concentrations ranging from 10^{11} to 10^{15} cm^{-3}. With increasing temperature, μ_H^{gas} decreases and exhibits a slight curvature. At the highest temperature, the rate of change of μ_H^{gas} decreases from -0.00178 eV K^{-1} for $C_H = 10^{15}$ cm^{-3} to -0.0026 eV K^{-1} for $C_H = 10^{11}$ cm^{-3}. On the other hand, for a given temperature μ_H^{gas} shows a linear dependence on C_H. This is depicted in the inset of Figure 1 for $T = 1000$ and 1700 K. Note that the slope changes for different temperatures.

During growth of a semiconductor, equilibration of the chemical potentials according to Equation (8) will cause H atoms to migrate from the growth chamber into the growing semiconductor because an ideal semiconductor would not contain H atoms. For this to happen, a necessary condition is the existence of empty sites to accommodate hydrogen. The nature of these sites depends on the host lattice and its properties. For example, in silicon possible H sites are the bond-center site for H^+,[16,17] the interstitial site for H^-,[18] and Si dangling bonds in vacancies or at stacking faults.[19] Also, hydrogen can form complexes with impurities and dopants,[2,3] and can even form large 2D defects known as platelets.[20] The sum of these states represents the hydrogen density-of-states, D_H. Thus, the total hydrogen concentration in a semiconductor is given by

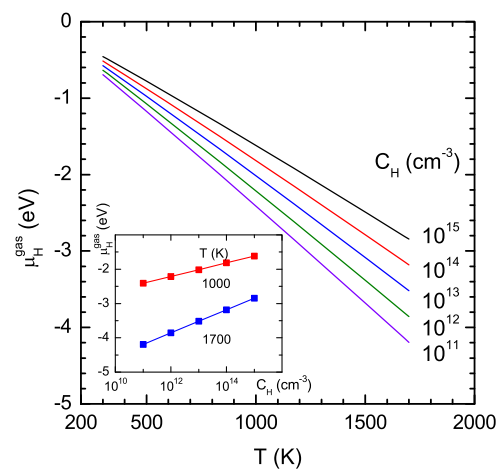$$C_H = \int_{-\infty}^{\infty} D_H(E) f(E, \mu_H, T) dE \tag{11}$$

Figure 1. Chemical potential, μ_H^{gas}, of a monatomic hydrogen gas for different hydrogen concentrations, C_H. The data were derived from Equation (9) and (10). The inset shows the position of the H chemical potential as a function of the H concentration for two different temperatures.

where E is the hydrogen binding energy and $f(E, \mu_H, T)$ is the occupation function.

3. Experimental Section

To reliably measure the H content even for low concentrations and to obtain information on H bonding, effusion measurements were performed. A schematic representation of the measurement setup is shown in **Figure 2**. Specimens with a size of about $1.0 \times 0.5\, cm^2$ were placed in ultrahigh vacuum. Then, the samples were heated with a heating rate of $20\, K\, min^{-1}$ while the flux of molecular hydrogen was measured with a quadrupole mass spectrometer. Background measurements were taken prior to the measurements and subtracted from the data. The ion current measured by the quadrupole mass spectrometer was calibrated to absolute values by using the known flux of neon through a capillary.

As representative samples commercially available, state-of-the-art semiconductors were chosen for the hydrogen effusion measurements, namely, 1) single-crystal silicon (c-Si) grown by the float-zone technique with a (100) surface orientation. The specimen was doped with a phosphorous concentration of $\approx 10^{12}\, cm^{-3}$ and had a thickness of $400\, \mu m$. For this growth method, high purity argon is used as a background gas. Often high purity nitrogen is added to minimize thermal ionization of Ar and improve electrical insulation to the heating coils.[21] 2) Single-crystal germanium (c-Ge) with a (111) surface orientation. This sample was grown by the Czochralski method that uses an inert atmosphere. The sample was doped with a gallium concentration of $\approx 10^{16}\, cm^{-3}$ and had a thickness of $350\, \mu m$. 3) Nominally undoped ZnO with a (0001) surface orientation and a thickness of $500\, \mu m$. One sample was grown hydrothermally (HT),[22] while the second ZnO crystal was grown using seeded physical vapor transport (CVT). For the HT growth process, a mixture of LiOH and KOH is used as mineralizers.[23] Hence, they are a likely source of hydrogen. On the other hand, the CVT growth process takes place in vacuum.[24] 4) Single-crystal melt-grown β-Ga$_2$O$_3$ with a (001) surface orientation. The sample was doped with a tin concentration of $1 \times 10^{18} - 2 \times 10^{19}\, cm^{-3}$ and had a thickness of

$650\, \mu m$. β-Ga$_2$O$_3$ crystals were grown from the melt under atmospheric pressure with a gas mixture of 98% N$_2$ and 2% O$_2$. After the growth the crystals were annealed in N$_2$ atmosphere to reduce strain and activate dopants.[25] The samples were not subjected to any further hydrogen treatment prior to the H effusion measurements.

4. Results and Discussion

In **Figure 3** the effusion rates of molecular hydrogen, dN_{H_2}/dt, are shown as a function of the annealing temperature, T. The elemental semiconductors exhibit significant H outdiffusion for $T > 500\, K$ with a similar onset of the effusion rate. c-Si shows a pronounced peak at $828\, K$, while for c-Ge the maximum effusion rate is less prominent and occurs at $845\, K$. The H effusion rates of the two oxides show a distinctly different behavior [Figure 3c,d]. Hydrogen effusion commences at lower temperatures, and at $T = 388$ and $409\, K$ peaks in the effusion rates are observed for β-Ga$_2$O$_3$ and ZnO, respectively. It is interesting to note that the H flux for CVT ZnO is more than one order of magnitude lower than for HT ZnO [see Figure 3b]. The origin of these low-temperature effusion peaks can be ascribed to residual water molecules on the surface of the samples. This is supported by the observation that effusion rates of O$_2$ and H$_2$O show peaks at the same temperatures.[26] Compared to the element semiconductors, both oxides exhibit more structure in the H$_2$ effusion rates. The maxima of dN_{H_2}/dt are observed at $T = 730$ and $660\, K$ for ZnO and β-Ga$_2$O$_3$, respectively.

The hydrogen concentration of the samples is obtained by integrating the effusion spectra according to

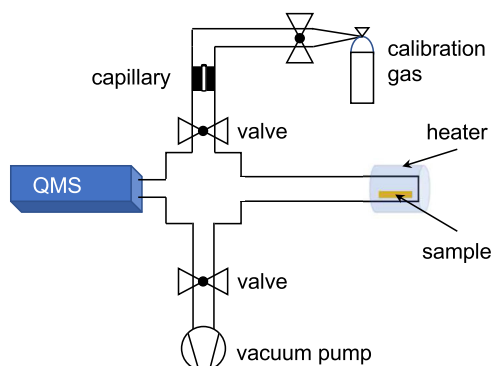$$C_H = \frac{2}{r_h d} \int \frac{dN_{H_2}}{dt} dT \qquad (12)$$

Figure 2. Schematic depiction of the hydrogen effusion system. The samples are placed in a quartz tube that is held at a base pressure of about 10^{-9} mbar. QMS denotes a quadrupole mass spectrometer. Experimental details are given in the text.
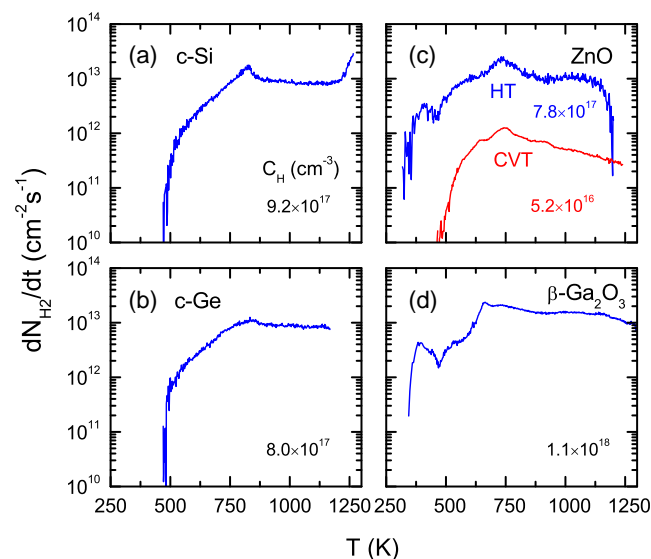

Figure 3. Effusion rate of molecular hydrogen, dN_{H_2}/dt, as a function of temperature. The data were obtained from a) c-Si, b) c-Ge, c) ZnO, and d) β-Ga$_2$O$_3$. For all measurements, the heating rate was $r_h = 20\, K\, min^{-1}$. C_H denotes the total H concentration obtained from Equation (12). Additional information on the samples is given in the text.

ADVANCED
SCIENCE NEWS
www.advancedsciencenews.com

physica
pss
status
solidi
b

www.pss-b.com

Here, d represents the sample thickness and r_h is the heating rate. The obtained values for C_H are indicated in Figure 3. It is interesting to note that C_H varies between 5.2×10^{16} and 1.1×10^{18} cm^{-3}. Hence, there is plenty of hydrogen present in the semiconductors that can influence the electronic properties by passivating defects such as vacancies and dislocations, neutralizing dopants, and forming complexes with impurities. It is interesting to note that float-zone c-Si, although electrically pure, contains a surprisingly high H concentration. Lower hydrogen concentrations can be achieved during crystal growth. For example, high-purity germanium crystals were grown in the past with a hydrogen concentration of 2×10^{15} cm^{-3}. To measure the H content, the isotope tritium was incorporated and monitored by its β-decay.[27] It is interesting to note that for β-Ga$_2$O$_3$ the H concentration agrees well with the reported net impurity concentration of $\approx 2 \times 10^{18}$ cm^{-3} giving rise to n-type conductivity. Originally, it was suggested that the n-type conductivity was caused by oxygen vacancies.[28]

The effusion spectra were further analyzed to relate C_H to the H chemical potential. Using the relation[29]

$$E_M - \mu_H(T) = -k_B T \ln\left(\frac{dN_{H_2}/dt}{N_0}\right) \tag{13}$$

the position of μ_H with respect to the migration saddle point, E_M, was determined. Note that μ_H is derived for molecular H. The prefactor for the gas effusion rate is defined as $N_0 \approx 2\nu a D_{surf}/d$, where ν is the attempt frequency, a is the mean free path for H migration, and D_{surf} is the number of surface states. Using an attempt frequency of $\approx 10^{13}$ s^{-1}, a mean free path of ≈ 3 Å, and a density of surface states of $\approx 10^{15}$ cm^{-2}, the effusion prefactor can be estimated to $d \times N_0 \approx 6 \times 10^{20}$ s^{-1} cm^{-1}. The prefactor is an average value. An error analysis for N_0 shows that even a change of one order of magnitude results in an error of only 100 meV for the position of μ_H.

Figure 4 shows the position of the H chemical potential with respect to the migration saddle point as a function of C_H for c-Si, c-Ge, ZnO, and β-Ga$_2$O$_3$. At high H concentrations ($C_H \approx 10^{18}$ cm^{-3}), $E_M - \mu_H$ resides at about -0.66 and -1 eV for the oxides and elemental semiconductors, respectively. As the H concentration decreases to $C_H \approx 7 \times 10^{17}$ cm^{-3}, the H chemical potential exhibits a rapid decrease. With further decreasing C_H, the decrease of $E_M - \mu_H$ becomes weaker until constant values of $E_M - \mu_H = -1.78, -2.16, -2.2$, and -2.29 eV are reached for ZnO, c-Ge, c-Si, and β-Ga$_2$O$_3$, respectively.

In semiconductors, the dependence of the H chemical potential on the hydrogen concentration is different compared to hydrogen in a gas. While μ_H^{gas} exhibits a monotonic decrease with decreasing C_H, in semiconductors the change of the H chemical potential with changing H concentration is governed by the H density-of-states distribution, D_H. This is similar to the Fermi energy of electrons, whose position is influenced by the electron density-of-states distribution. From the H effusion spectra, D_H can be derived. The total H concentration and D_H are related by Equation (11). Partial differentiation of Equation (11) yields D_H. Since the occupation function $f(E, \mu_H, T)$ shows a peak for $E = \mu_H$, the H density-of-states distribution is given by[29]

$$D_H(\mu_H) \approx \frac{\partial C_H}{\partial \mu_H} \tag{14}$$

The resulting H density-of-states distributions for the investigated semiconductors are plotted in **Figure 5**. c-Si and c-Ge exhibit a single peak at $E_M - \mu_H = -1.42$ and -1.44 eV, respectively, that is followed by a broader plateau. In contrast, the oxide semiconductors show more structure in the H density-of-states. ZnO exhibits a prominent peak at $E_M - \mu_H = -1.20$ eV and two relatively broad peaks centered at $E_M - \mu_H = -0.95$ and -1.76 eV for HT samples that shift to lower energies for CVT ZnO. On the other hand, a needle-like peak is observed for
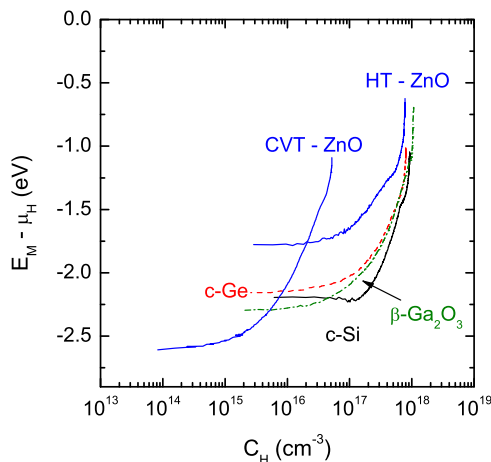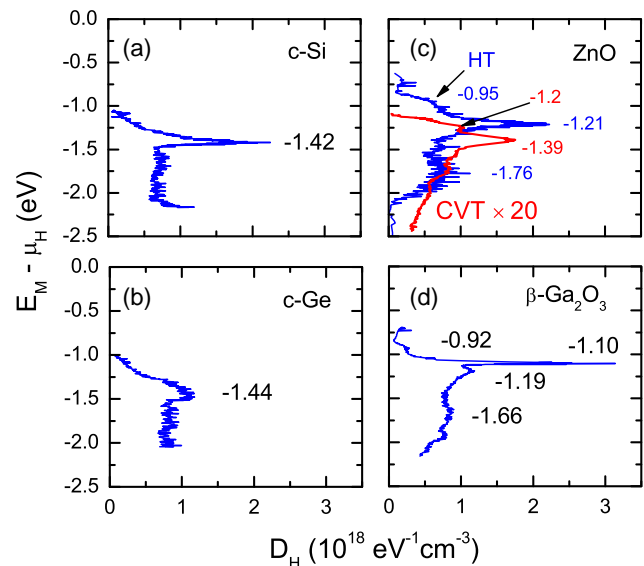

Figure 4. Position of the H chemical potential with respect to the migration saddle point, $E_M - \mu_H$, as a function of C_H for c-Si, c-Ge, ZnO, and β-Ga$_2$O$_3$. The data were obtained from the effusion spectra by employing Equation (13).

Figure 5. Hydrogen density-of-states distribution, D_H, in state-of-the-art a) c-Si, b) c-Ge, c) single-crystal ZnO, and d) single-crystal β-Ga$_2$O$_3$. The numbers in the figure indicate the peak energies. The data were derived from the H effusion spectra shown in Figure 3.

ADVANCED
SCIENCE NEWS
www.advancedsciencenews.com

physica pssb
status solidi

www.pss-b.com

β-Ga$_2$O$_3$ at $E_M - \mu_H = -1.10$ eV. This is reminiscent of Guinier–Preston zones in metal alloys.[30] Furthermore, some less pronounced peaks are located at $E_M - \mu_H = -0.92$, -1.19, and -1.66 eV.

Although the properties of hydrogen in semiconductors have been extensively researched in the past, an assignment of the peaks of the H density-of-states to specific hydrogen complexes is difficult. In the past, numerous H-related complexes such as O–H in ZnO[31] and β-Ga$_2$O$_3$,[32] or H-passivated vacancies and H-impurity complexes in silicon[33] and germanium[34] were identified experimentally. However, to assign peaks in the density-of-states to specific complexes requires direct correlations using methods that allow chemical identification.

5. Summary

In summary, a theoretical framework based on thermodynamics was presented that accounts for the incorporation of hydrogen during growth even in high purity semiconductors. A likely source for H is residual water vapor in the growth chamber. Effusion measurements performed on state-of-the-art c-Si, c-Ge, CVT, and HT ZnO, and β-Ga$_2$O$_3$ revealed H concentrations of 9.2×10^{17}, 8×10^{17}, 5.2×10^{16} to 7.8×10^{17}, and 1.1×10^{18} cm^{-3}, respectively. From the effusion spectra, $E_M - \mu_H$ and the hydrogen density-of-states distributions were determined. In elemental semiconductors, H is more strongly bound than in ZnO and β-Ga$_2$O$_3$. On the other hand, the H density-of-states exhibits needle-like peaks at -1.1, and -1.2 eV for β-Ga$_2$O$_3$ and ZnO, respectively.

Acknowledgements

Conflict of Interest

The author declares no conflict of interest.

Data Availability Statement

The data that support the findings of this article are available from the author upon reasonable request.

Keywords

[1] G. Alefeld, J. Völkl, *Hydrogen in Metals I*, Topics in Applied Physics, Vol. 28, Springer, Berlin **1978**.
[2] J. I. Pankove, N. M. Johnson, *Hydrogen in Semiconductors*, Semiconductors and Semimetals, Vol. 34, Academic Press, San Diego **1991**.
[3] N. H. Nickel, in *Hydrogen In Semiconductors II*, Semiconductors and Semimetals, Vol. 61, Academic Press, San Diego **1999**.
[4] J. R. Ritter, J. Huso, P. T. Dickens, J. B. Varley, K. G. Lynn, M. D. McCluskey, *Appl. Phys. Lett.* **2018**, *113*.
[5] R. Nakayama, M. Maesato, G. Lim, M. Arita, H. Kitagawa, *J. Am. Chem. Soc.* **2021**, *143*, 6616.
[6] N. H. Nickel, K. Geilert, *Appl. Phys. Lett.* **2020**, *116*, 242102.
[7] N. H. Nickel, K. Geilert, *J. Appl. Phys.* **2021**, *129*, 195704.
[8] B. Clerjaud, *Physica B* **1991**, *170*, 383.
[9] S. J. Pearton, H. Cho, F. Ren, J. I. Chyi, J. Han, R. G. Wilson, *MRS Internet J. Nitride Semicond. Res.* **2000**, *5*, 540.
[10] C. G. Van De Walle, J. Neugebauer, *Nature* **2003**, *423*, 626.
[11] C. Herring, N. Johnson, C. Van de Walle, *Phys. Rev. B* **2001**, *64*, 125209.
[12] C. G. Van de Walle, J. Neugebauer, *J. Appl. Phys.* **2004**, *95*, 3851.
[13] H. H. G. Jellinek, *J. Chem. Educ.* **1986**, *63*, 1029.
[14] C. I. M. Beenakker, F. J. D. Heer, H. B. Krop, G. R. Möhlmann, *Chem. Phys.* **1974**, *6*, 445.
[15] C. Kittel, *Thermal Physics*, Wiley, New York **1969**, p. 164.
[16] C. G. Van de Walle, P. J. H. Denteneer, Y. Bar-Yam, S. T. Pantelides, *Phys. Rev. B* **1989**, *39*, 10791.
[17] Yu. V. Gorelkinskii, N. N. Nevinnyi, *Sov. Tech. Phys. Lett.* **1987**, *13*, 45 [*Pis'ma Zh. Tekh. Fiz. (USSR)* **1987**, 13, 105].
[18] N. M. Johnson, C. Herring, C. G. Van de Walle, *Phys. Rev. Lett.* **1994**, *73*, 130.
[19] J. E. Lawrence, *J. Appl. Phys.* **1969**, *40*, 360.
[20] N. M. Johnson, F. A. Ponce, R. A. Street, R. J. Nemanich, *Phys. Rev. B* **1987**, *35*, 4166.
[21] F. Zobel, Dissertation, Univ. Halle-Wittenberg **2018**.
[22] M. Suscavage, M. Harris, D. Bliss, P. Yip, S.-Q. Wang, D. Schwall, L. Bouthillette, J. Bailey, M. Callahan, D. C. Look, D. C. Reynolds, R. L. Jones, C. W. Litton, *MRS Internet J. Nitride Semicond. Res.* **1999**, *4*, 287.
[23] K. Maeda, M. Sato, I. Niikura, T. Fukuda, *Semicond. Sci. Technol.* **2005**, *20*, S49.
[24] S. H. Hong, M. Mikami, K. Mimura, M. Uchikoshi, A. Yasuo, S. Abe, K. Masumoto, M. Isshiki, *J. Cryst. Growth* **2009**, *311*, 3609.
[25] A. Kuramata, K. Koshi, S. Watanabe, Y. Yamaoka, T. Masui, S. Yamakoshi, *Jpn. J. Appl. Phys.* **2016**, *55*, 1202A2.
[26] N. H. Nickel, unpublished data.
[27] W. L. Hansen, E. E. Haller, P. N. Luke, *IEEE Trans. Nucl. Sci.* **1982**, *NS-29*, 738.
[28] M. R. Lorenz, J. F. Woods, R. J. Gambino, *J. Phys. Chem. Solids* **1967**, *28*, 403.
[29] W. B. Jackson, A. J. Franz, H. C. Jin, J. R. Abelson, J. L. Gland, *J. Non-Cryst. Solids* **1998**, *227–230*, 143.
[30] J. B. Cohen, *Solid State Phys.* **1986**, *39*, 131.
[31] S. J. Jokela, M. D. McCluskey, *Phys. Rev. B* **2005**, *72*, 113201.
[32] P. Weiser, M. Stavola, W. B. Fowler, Y. Qin, S. Pearton, *Appl. Phys. Lett.* **2018**, *112*, 232104.
[33] R. Jones, B. J. Coomer, J. P. Goss, B. Hourahine, A. Resende, *Diffus. Defect Data, Pt.B: Solid State Phenom.* **2000**, *71*, 173.
[34] J. Weber, M. Hiller, E. V. Lavrov, *Mater. Sci. Semicond. Process.* **2006**, *9*, 564.